

UNCLASSIFIED



Australian Government

Department of Defence

Science and Technology

CTH Implementation of a Two-Phase Material Model with Damage

Anatoly D. Resnyansky

Weapons and Combat Systems Division

Defence Science and Technology Group

DST-Group-TR-3539

ABSTRACT

A material model taking strength and damage accumulation into account is implemented in the CTH hydrocode. The model is based on a two-phase approach with the phases representing virgin and fully crushed material states with individual strength and elastic characteristics. Multi-phase description is realised via a homogenisation procedure representing a damaging material as a mixture of the phases, which results in an equation of state, constitutive equations, and conservation laws. The implementation has been used for numerical modelling of high velocity impact against targets made of generic materials representing glass and concrete. The calculations illustrate the dominating effect of the damage mode specified by material.

RELEASE LIMITATION

Approved for public release

UNCLASSIFIED

UNCLASSIFIED

Produced by

*Weapons and Combat Systems Division
Defence Science and Technology Group
PO Box 1500
Edinburgh SA 5111*

Telephone: 1300 333 362

*© Commonwealth of Australia 2018
October 2018*

APPROVED FOR PUBLIC RELEASE

UNCLASSIFIED

UNCLASSIFIED

CTH Implementation of a Two-Phase Material Model with Damage

Executive Summary

Critical materials used in civilian and military applications (high-speed vehicles, warheads, and military protection) are often brittle materials such as structural materials (concretes), glasses, and ceramics. The rate sensitivity of conventional and advanced materials is one of the driving factors in the development of novel constitutive models. At the same time, geological brittle materials are extremely sensitive to the loading modes resulting in dramatically different response to compression, tension, or shear.

For enhancement of the DST Group modelling capability against impact threats in structural and other brittle materials, an advanced model analysing material damage response to different strain rates and modes of loading has been developed [1] and implemented in a hydrocode. In the present work, this model is reformulated to decouple the bulk and shear response of materials, which is convenient for implementation in the CTH hydrocode. This shock physics modelling code is available in DST Group and has an extended material model database enabling the user to evaluate a number of weapons and protection systems. Numerical examples considered with the present implementation demonstrate that the model is capable of describing both the fracture waves associated with the compression mode of loading in glasses and the damage characterised by frontal scabbing and rear spallation associated with the shear mode of loading in concretes.

Reference

[1] A.D. Resnyansky, E.I. Romensky, and N.K. Bourne, Constitutive Modeling of Fracture Waves, *J. App. Physics*, 2003, 93 (3), pp. 1537-1545.

UNCLASSIFIED

UNCLASSIFIED

This page is intentionally blank.

UNCLASSIFIED

Author

Anatoly D. Resnyansky
Weapons and Combat Systems Division

Anatoly Resnyansky obtained a Masters of Science in Applied Mathematics and Mechanics from Novosibirsk State University (Russia) in 1979. In 1979-1995 he worked in the Laorentyev Institute of Hydrodynamics (Russian Academy of Science) in the area of constitutive modelling for problems of high-velocity impact. Anatoly obtained a PhD in Physics and Mathematics from the Institute of Hydrodynamics in 1985. He joined the Terminal Effects (presently Warhead Effects) Group of the Weapons Systems Division in DSTO (presently Weapons and Combat Systems Division in DST Group) in 1998. Anatoly was appointed Adjunct Professor at University of South Australia in 2014. His current research interests include constitutive modelling and material characterisation at high strain rates, and theoretical and experimental analysis of multi-phase flows. He has published over one hundred research and technical papers.

UNCLASSIFIED

This page is intentionally blank.

UNCLASSIFIED

Contents

1. INTRODUCTION.....	1
2. BACKGROUND.....	3
3. EQUATION OF STATE.....	5
4. CONSTITUTIVE EQUATIONS.....	7
5. CTH IMPLEMENTATION.....	9
5.1 Input Block.....	9
5.1.1 UINEP modifications	10
5.1.2 EOSVEI modifications	11
5.1.3 UINCHK modifications.....	11
5.1.4 UINISV modifications.....	11
5.1.5 EOSVEK modifications.....	12
5.2 Lagrangian Block	12
5.2.1 ELSG modifications.....	12
5.3 Eulerian Remap Block.....	13
5.3.1 EOSVEV and EOSVES modifications	13
5.3.2 EOSVEX modifications	13
5.3.3 EREB modifications.....	13
6. NUMERICAL EXAMPLES	14
7. CONCLUSIONS.....	16
8. REFERENCES	17

UNCLASSIFIED

DST-Group-TR-3539

This page is intentionally blank.

UNCLASSIFIED

1. Introduction

There are a number of material models implemented in hydrocodes describing fracture of brittle materials, including concretes, under dynamic loading. Specifically, the model database of the shock physics CTH hydrocode [1] includes such models as Holmquist-Johnson-Cook model [2] (HJC model [1]), Brittle Fracture Kinetics model [3] (BFK model [4]), Pressure-Shear damage model based on [5] (PSDam model [6]). As an example, these models can be utilized for description of concrete response against impact threats. However, when, applying the HJC model [7] or PSDam model to data [8] the simulations evaluate the total damage (damage volume) reasonably well, but they frequently could not adequately describe the damage propagation directions and damage patterns [8]. In addition, the simulations require a significant number of fitting parameters with uncertain physical background. Therefore, the constitutive material model [9] is explored in the present work.

Previous implementation of the present model [9] in the LS-Dyna hydrocode [10] was successfully employed for description of the impact response of filled glass materials [11, 12]. However, the Eulerian CTH hydrocode enables one to address a wider variety of targets and material models, which are important for evaluation of the countermeasure effectiveness of targets against high velocity projectiles and blast loads and performance of weapons. Therefore, an implementation of the model in the CTH hydrocode is required, which is convenient when bulk and deviatoric responses of material are decoupled [13]. Reformulation of the model [9] into the decoupled form is outlined in the next section. Introduction of virgin and crushed phases of damaged material requires linkages between parameters of the phases and the mixture. Application of a homogenisation procedure of a two-phase averaged mixture representing a damaged material results in linkages between thermodynamic parameters of the mixture with those of the virgin and crushed phases. These linkages, equations of state for the phases, and an additivity mixture rule for a thermodynamic potential enables us to derive an equation of state (EOS) for the damaged material as outlined in the 'Equation of State' section.

Using the governing laws for the phases and rate sensitive constitutive equations for phase plasticity describing evolution of deviatoric elastic deformations, the parameter linkages allow us to derive the rate sensitive constitutive equations accounting for the material strength evolution. The volume concentration parameter for the crushed phase can be seen as a parameter responsible for damage accumulation. Constitutive equations for this parameter are responsible for degradation of yield stress and elastic moduli of the damaged material. These equations close the model and they are outlined in the 'Constitutive Equations' section.

The CTH implementation of the present model is described in the 'CTH Implementation' section. Typical CTH implementation deals with three groups of subroutines in the code. The present implementation includes modifications to i) the input subroutines in the elasto-plastic (EP) input part of the code, ii) evaluation of deviatoric stresses in the Lagrangian part; and iii) recalculation of pressure, energy, and temperature using EOS in the Eulerian Remap part of the CTH code.

The implemented code is used for calculation of the examples of modelling fracture waves in glasses based on a high-velocity impact set-up [9] and a ballistic impact against concrete target within a set-up [8]. In the case of impact against a block of glass the dominant failure mechanism is pressure driven and is observed in experiments as propagation of fracture waves. On the contrary, in the case of penetration of concretes, including a high performance concrete, the dominant mode of fracture is shear and it is seen in experimental observations as extensive front scabbing and rear spallation. Adequate dependence of the character of fracture on the choice of the loading modes in each of the cases is demonstrated in the 'Numerical Examples' section by corresponding CTH modelling results.

2. Background

The two-phase approach [9] considers a brittle material subjected to damage as a two-phase mixture of two hypothetical constituents that represent i) the material in its original state ('virgin' phase or phase '1') with strength corresponding to the supplied material and ii) a hypothetical material in fully damaged state ('crushed' phase or phase '2') with residual strength associated with a reduced bearing capacity of the material in this state. Concentration of the crushed phase, c , is a constitutive parameter that can be associated with accumulation and propagation of damage. Thus, the state of the material may vary from virgin state ($c = 0$) to fully crushed state ($c = 1$) evolving via intermediate states ($0 < c < 1$).

Application of the homogenisation procedure [9] to the mass, momentum, and energy balance laws for the phases results in conventional conservation laws for mass, momentum, and energy for the mixture. In turn, the constitutive equations for deviatoric elastic deformations for the phases are the basis for derivation of the corresponding constitutive equation for the mixture employing the homogenisation procedure rules. Finally, the value of the phase concentration for the crushed phase can be associated with accumulated damage, which generates the last constitutive equation.

Focusing on parameters specifying the state of the material, the system of equations describes the evolution of standard thermodynamic variables, specifically, e - specific internal energy (thermodynamic potential used with the chosen set of independent thermodynamic variables), ρ - density, p - pressure, and kinematic variables (velocity components) u_i . These parameters describe a state of the two-phase mixture representing a damaged material. Strength response is described by mass weighted small elastic deviatoric strains of the mixture, $e_{ij} = \varepsilon_{ij}'/\rho$, where deviatoric components of the tensor of small elastic strains, ε_{ij} , are

$$\varepsilon_{ij}' = \varepsilon_{ij} - (\varepsilon_{11} + \varepsilon_{22} + \varepsilon_{33}) \delta_{ij}/3 ,$$

here δ_{ij} are components of the unit tensor. The tensor e_{ij} is introduced in order to provide a description of the strength response of the material within the framework of decoupling bulk and deviatoric responses [13] based on the uncoupled Maxwell-type viscoelastic material model [14]. Having introduced the deviatoric strain response, the bulk response is characterised by density change and the full strain tensor can be represented as follows

$$\varepsilon_{ij} = \varepsilon_{ij}' + (\varepsilon_{11} + \varepsilon_{22} + \varepsilon_{33}) \delta_{ij}/3 = \rho e_{ij} + \ln(\rho_0/\rho) \cdot \delta_{ij}/3 \quad (1)$$

Similar decomposition for the stress tensor takes the following form

$$\sigma_{ij} = \sigma_{ij}' - (\sigma_{11} + \sigma_{22} + \sigma_{33}) \delta_{ij}/3 = s_{ij} + p \cdot \delta_{ij}/3 \quad (2)$$

where s_{ij} denotes components of the stress deviator and $p = - (\sigma_{11} + \sigma_{22} + \sigma_{33}) \delta_{ij}/3$ - pressure.

Thus, replacing conventional stress and strain variables in the system of equations of the model [9] with the decoupling sets of variables from (1) and (2), the system of conservation laws and a set of constitutive equations accounting for strength (see [13]), completed with the kinetic equation for the damage concentration parameter c , responsible for accumulation and evolution of damage form the following system compatible with the damage model [9] and the bulk-shear decoupling approach [13]:

$$\begin{aligned} \frac{\partial \rho}{\partial t} + \frac{\partial \rho u_k}{\partial x_k} = 0, \quad \frac{\partial \rho u_i}{\partial t} + \frac{\partial (\rho u_i u_j - s_{ij})}{\partial x_j} + \frac{\partial p}{\partial x_i} = 0, \quad \frac{\partial \rho E}{\partial t} + \frac{\partial (\rho u_j E - s_{ij} u_i + p u_j)}{\partial x_j} = 0, \\ \frac{\partial \rho e_{ij}}{\partial t} + \frac{\partial \rho u_k e_{ij}}{\partial x_k} - \frac{\partial u_i/2}{\partial x_j} - \frac{\partial u_j/2}{\partial x_i} + \frac{\partial u_k/3}{\partial x_k} \cdot \delta_{ij} = -\rho \varphi_{ij}, \quad \frac{\partial \rho c}{\partial t} + \frac{\partial \rho c u_i}{\partial x_i} = -\rho \psi, \end{aligned} \quad (3)$$

here $E = e + |u|^2/2$ and the constitutive functions φ_{ij} and ψ will be specified later. Dependant thermodynamic parameters such as pressure, stresses, temperature, T , and a structural stress, q , associated with damage c (see [9]), are linked with independent parameters of density, elastic strains, specific entropy S , and damage via the thermodynamic potential $e = e(\rho, e_{ij}, c, S)$, employing the thermodynamic identity $TdS = de + pdV - s_{ij}de_{ji} - qdc$, where specific volume $V = 1/\rho$, as follows

$$p = \rho^2 \partial e / \partial \rho, \quad s_{ij} = \partial e / \partial e_{ji}, \quad T = \partial e / \partial S, \quad q = \partial e / \partial c. \quad (4)$$

The additivity mixture rule is applied to density, total internal energy $U = \rho e$, strain and total entropy $s = \rho S$, which takes the following form [9]:

$$\begin{aligned} \rho &= (1 - c) \rho^{(1)} + c \rho^{(2)}, \quad U = (1 - c) U^{(1)} + c U^{(2)}, \\ \varepsilon_{ij} &= (1 - c) \varepsilon_{ij}^{(1)} + c \varepsilon_{ij}^{(2)}, \quad s = (1 - c) s^{(1)} + c s^{(2)}. \end{aligned}$$

Stresses, temperature, and kinematic parameters (velocity components) are assumed to be in inter-phase equilibrium [9].

3. Equation of State

Using internal energy potentials for the phases, EOS for the damaging material can be obtained from the mixture rule of the previous Section and written in the abovementioned form $e = e(\rho, e_{ij}, c, S)$. EOS for the mixture can be restored from given laws for stress and temperature, using the consequences (4) of the thermodynamic identity. As a first approximation, linear relations are assumed for the force and temperature characteristics against small elastic deformations ε_{ij} and specific entropy for the two phases as in [9]:

$$\sigma_{ij} = K(\varepsilon_{11} + \varepsilon_{22} + \varepsilon_{33})\delta_{ij} + 2G\varepsilon_{ij}' - \pi\rho S\delta_{ij}, \quad T = T_0 + \omega\rho S - \pi(\varepsilon_{11} + \varepsilon_{22} + \varepsilon_{33}), \quad (5)$$

where indices '1' and '2' which refer the parameters to the phase numbers are omitted for simplicity. Here, K and G are bulk and shear modulus, $\pi = \gamma T_0$, $\omega = T_0/(\rho_0 c_v)$, T_0 and ρ_0 are reference temperature and density, γ is the Grüneisen coefficient, and c_v is specific heat.

Replacing stress and strain variables by the variables consistent with the decoupling procedure, following the homogenisation rules [9], and applying some linearisation for consistency with (4), the relations similar to (5) for the two-phase mixture are obtained from (5) as follows

$$p = K(\rho/\rho_0) \ln(\rho/\rho_0) + P\rho S, \quad s_{ij} = 2G\rho_0 e_{ij}, \quad T = T_0 + \Omega\rho_0 S + P \ln(\rho/\rho_0). \quad (6)$$

Here, K , G , P , and Ω without indices are the corresponding moduli for the mixture [9] derived from the homogenisation rules:

$$\begin{aligned} K &= \frac{K_1'K_2'}{\tilde{K}'} + \frac{\pi_1\pi_2}{\tilde{\omega}'}, \quad G = \frac{G_1G_2}{\tilde{G}}, \quad P = \left\langle \frac{\pi}{\omega} \right\rangle \frac{\omega_1\omega_2}{\tilde{\omega}} - \left\langle \frac{\pi'}{K'} \right\rangle \frac{K_1'K_2'}{\tilde{K}'}, \\ \Omega &= \frac{\omega_1\omega_2}{\tilde{\omega}} - \left\langle \frac{\pi'}{K'} \right\rangle^2 \frac{K_1'K_2'}{\tilde{K}'} - \left\langle \frac{(\pi')^2}{K'} \right\rangle, \end{aligned} \quad (7)$$

where

$$\begin{aligned} \tilde{a} &= ca_1 + (1-c)a_2, \quad \langle a \rangle = (1-c)a_1 + ca_2, \\ K_i' &= K_i - \frac{\tilde{\pi}}{\tilde{\omega}} \pi_i, \quad \omega_i' = \omega_i - \frac{\tilde{\pi}}{\tilde{K}} \pi_i, \quad \pi_i' = \pi_i - \frac{\tilde{\pi}}{\tilde{\omega}} \omega_i, \quad i=1,2. \end{aligned}$$

Following (4), the corresponding EOS (internal energy potential) in the linearised form for the mixture is taken as follows

$$e = K [\ln(\rho/\rho_0)]^2/(2\rho_0) + \rho_0 G J_e + P \ln(\rho/\rho_0) S + \rho_0 \Omega S^2/2 + T_0 S, \quad (8)$$

here J_e is proportional to the second invariant of the e_{ij} tensor:

$$J_e = e_{11}^2 + e_{22}^2 + e_{33}^2 + 2(e_{12}e_{21} + e_{23}e_{32} + e_{31}e_{13}). \quad (9)$$

For numerical illustrations of this work described in Section 6 below, the following EOS parameters were selected for the case of glass material:

$$\rho_{01} = \rho_{02} = 2.23 \text{ g/cm}^3; K_1 = 81.6 \text{ GPa}; K_2 = 81.6 \text{ GPa}; G_1 = 30 \text{ GPa}; G_2 = 7.6 \text{ GPa};$$

$$c_{v1} = c_{v2} = 1.0 \text{ J/(g} \cdot \text{K)}; \gamma_1 = \gamma_2 = 1.9 .$$

Similarly, for the concrete material

$$\rho_{01} = \rho_{02} = 2 \text{ g/cm}^3; K_1 = 16.8 \text{ GPa}; K_2 = 4.2 \text{ GPa}; G_1 = 13 \text{ GPa}; G_2 = 0.5 \text{ GPa};$$

$$c_{v1} = c_{v2} = 0.9 \text{ J/(g} \cdot \text{K)}; \gamma_1 = \gamma_2 = 0.9 .$$

Thus, the EOS (8) along with the relationships obtained from (4) close the system of equations (3) of the models if the kinetic functions φ_{ij} and ψ are specified.

4. Constitutive Equations

Using the constitutive equations for deviatoric elastic deformations of the phases and the linkages between the phase-specific and averaged elastic deformations, the corresponding constitutive equations for the mixture can be derived [9]. The homogenisation results in the constitutive equations (equations for e_{ij} in (1)) of the same form as those for the phases. However, the constitutive functions φ_{ij} vary with the damage accumulation parameter, while degenerating to the equations for the virgin or crushed phases depending on the value of the parameter. These equations are derived [9] from the corresponding viscoelastic equations for the phases. Schematically, they are reduced (with linearisation over density) to the following equations for stresses s_{ij} directly used in the CTH constitutive block:

$$\frac{ds_{ij}}{dt} - 2GD_{ij} = -2G\varphi_{ij}, \quad (10)$$

where $d/dt = \partial/\partial t + u_k \partial/\partial x_k$ denotes the substantial derivative and D_{ij} is the strain rate deviatoric tensor. Viscoelastic response for each of the phases is characterised by the shear stress relaxation time functions $\tau = \exp(a - b\sigma^e)$ (again, omitting indices for τ , a , and b referring to the phases), where σ^e is an effective stress $\sigma^e = (3J_\sigma/2)^{1/2}$. For the phases ($k = 1,2$), the generating equations similar to (6) are [14]:

$$\frac{ds_{ij}^{(k)}}{dt} - 2G_k D_{ij} = -\frac{s_{ij}^{(k)}}{\tau_k}. \quad (11)$$

The procedure for determination of the constants a_k and b_k from two yield limits Y (Y_1, Y_2 for the virgin phase and Y_{1d}, Y_{2d} for the crushed phase) at two different strain rates $d\varepsilon/dt$ (at 10^{L1} and 10^{L2} inverse seconds, respectively) is described in [13] for the 'time relaxation' functions responsible for the rate sensitivity of the yield limits:

$$\tau_k(s) = \exp\left[\left(a_k - b_k s^{(k)}\right)\right], \quad (12)$$

where, $(s^{(k)})^2 = s_{ij}^{(k)} s_{ij}^{(k)}$. The shear moduli are specified for virgin (G_1) and crushed (G_2) phases.

Then, as found in [9], the kinetic functions for the kinetic equation (6) are

$$\varphi_{ij} = \frac{s_{ij}}{2} \left(\frac{1-c}{G_1 \tau_1} + \frac{c}{G_2 \tau_2} \right). \quad (13)$$

Thus, pre-given functions $\tau^{(k)}(s)$ ($k = 1,2$) fully specify the kinetic functions φ_{ij} , closing the system of constitutive equations (1) of the model for strength. The damage constitutive function ψ is determined from the last constitutive equation in the system (1) that can be rewritten as

$$\frac{dc}{dt} = -\psi . \quad (15)$$

The equation employs the following slightly modified kinetic function [9]

$$\psi = A_{c0}(c + c_\varepsilon)(1 - c)q\psi_0 , \quad (16)$$

where c_ε is a small parameter, q is the structural stress from (2), and ψ_0 is taken as follows

$$\psi_0 = (1 - c) \left| \frac{\sigma}{\sigma_*} \right|^n + c \left| \frac{\sigma}{\sigma_0} \right| , \quad \sigma = A_S H(\sigma_{\max} - \sigma_{\min} - \sigma_p) \sigma^e + A_P H(p) p . \quad (17)$$

Here H is the Heaviside step function, σ_{\min} and σ_{\max} are minimal and maximal principal stresses, A_S and A_P are parameters informing which mode of loading is the most relevant for a given material, and A_{c0} , σ_* , σ_0 , σ_p are input parameters. If $\sigma < \sigma_{\text{crit}}$, the function ψ is reduced to $\psi = A_{c0}c_\varepsilon q/\rho$.

The constants a_k and b_k ($k = 1, 2$) of the strength constitutive equation (10) for the time relaxation functions $\tau^{(k)}$ can be obtained from pre-given yield limits of the virgin and crushed phases of the damaged materials considered. For the calculations below simulating damage in the glass materials these yield limits are specified as follows

$$Y_1 = 1.2 \text{ GPa}, Y_{1d} = 120 \text{ MPa at } d\varepsilon/dt = 10 \text{ s}^{-1}; Y_2 = 1.6 \text{ GPa}, Y_{2d} = 160 \text{ MPa at } d\varepsilon/dt = 10^3 \text{ s}^{-1}.$$

For the damage calculations of concrete these yield limits are taken as

$$Y_1 = 50 \text{ MPa}, Y_{1d} = 5 \text{ MPa at } d\varepsilon/dt = 10^{-1} \text{ s}^{-1}; Y_2 = 100 \text{ MPa}, Y_{2d} = 10 \text{ MPa at } d\varepsilon/dt = 10^3 \text{ s}^{-1}.$$

Parameters of the damage kinetics (15) are selected by accounting for the dominant mode of failure. For the glass material that is prone to failure dominated by compression, the damage kinetics constants are taken as follows

$$c_\varepsilon = 10^{-16}, \sigma_{\text{crit}} = 2 \text{ GPa}, A_{c0} = 10^3 \text{ s}^2 / (\text{K} \cdot \text{cm}^3), \sigma_* = 1.7 \text{ GPa}, \sigma_0 = 8 \text{ MPa}, \sigma_p = 2 \text{ GPa} ,$$

$$n = 32.5, A_S = 0.3, A_P = 0.9.$$

Similarly, for the concrete material that is prone to failure dominated by shear, the corresponding constants are

$$c_\varepsilon = 10^{-10}, \sigma_{\text{crit}} = 15 \text{ MPa}, A_{c0} = 10^3 \text{ s}^2 / (\text{K} \cdot \text{cm}^3), \sigma_* = 200 \text{ MPa}, \sigma_0 = 60 \text{ MPa}, \sigma_p = 20 \text{ MPa} ,$$

$$n = 20.1, A_S = 1.0, A_P = 0.$$

Thus, the model is fully specified with the constitutive function completing the equations of state specified in the preceding section.

5. CTH Implementation

A number of subroutine modifications were required for implementation of the model. Summary of the CTH subroutine modifications are:

1. initializing elasto-plastic input in UINEP complemented with a limited EOS input (initial material density) in the subroutine EOSVEI required for initial start of EOS subroutines
2. parameter check in UINCHK (subroutine VEDCHK)
3. definition of extra variables for the elasto-plastic set in UINISV (subroutine VEDEXV) and duplicating this set as EOS variables with the subroutine EOSVEK
4. fracture criterion input in UINFCK
5. EOS calculations of thermodynamic parameters (the subroutine EOSVES of EOSMGRE subroutine) based on density and temperature and those (the subroutine EOSVEV of EOSMGRE subroutine) based on density and energy
6. calculation of internal energy (the subroutine EOSVEX called by ELEX subroutine) subject to updated extra variables
7. calculation of the strength constitutive equation in the ELSG subroutine (subroutine VEDDRV calling subroutine VEDSIG and update of deviatoric stresses using the relaxation equation (6) coded in subroutine VEDRLX) and damage equation (update of the damage parameters using equation (7) coded in subroutine VEDEXD called by subroutine VEDSIG);
8. update of the invariant J_e in the Eulerian subroutine EREB; and
9. exchange of extra variables between the elasto-plastic and EOS sets in Lagrangian subroutine ELEB (subroutine VEDSWP).

It should be noted that modifications in the EOS block are performed via substitutions into available subroutines of the 'VE' (visco-elastic model in CTH) model (the subroutines with the names beginning with 'EOSVE'). The present implementation affects the following three CTH blocks: Input Block, Lagrangian Block, and Eulerian Remap Block modules and outlined in more details below for the affected subroutines.

5.1 Input Block

For the first Input Block, three Lagrangian Block subroutines [15-17] were involved in the modifications, namely, UINEP.FOR, UINCHK.FOR, and UINISV.FOR. The EOS input is only partly accessible via the subroutine EOSVEI of a substitute VE model of the CTH code.

5.1.1 UINEP modifications

UINEP.FOR modifications read in the data from the VP_data input file into the VPUINP array allocated for the EP related input data [17]. The data needed for the model input are: 'R01', 'R02', 'C01', 'C02', 'B01', 'B02', 'GM1', 'GM2', 'CV1', 'CV2', 'LGEP1', 'LGEP2', 'Y1', 'Y2', 'Y1D', 'Y2D', 'CEPA', 'AKOS', 'AKOP', 'AP0', 'SCRT', 'AN1', 'SGC1', 'SGC2', 'REC', 'PRS0', and 'YST'.

The most important information for a user is definition of the input parameters, when describing the elasto-plastic input. The input parameters for the model are listed below

R01 - initial density of the virgin phase
 C01 - initial bulk sound velocity of the virgin phase
 B01 - initial shear sound velocity of the virgin phase
 GM1 - Grüneisen parameter of the virgin phase
 CV1 - specific heat of the virgin phase
 R02 - initial density of the damaged phase
 C02 - initial bulk sound velocity of the damaged phase
 B02 - initial shear sound velocity of the damaged phase
 GM2 - Grüneisen parameter of the damaged phase
 CV2 - specific heat of the damaged phase
 LGEP1 - exponent L1 determining the first strain rate for rate sensitive strength
 LGEP2 - exponent L2 determining the second strain rate for rate sensitive strength
 Y1 - yield limit Y_1 corresponding to the first strain rate for the virgin phase
 Y2 - yield limit Y_2 corresponding to the second strain rate for the virgin phase
 Y1D - yield limit Y_{1d} corresponding to the first strain rate for the damaged phase
 Y2D - yield limit Y_{2d} corresponding to the second strain rate for the damaged phase
 CEPA - small parameter c_ϵ in the damage kinetic (8)
 AKOS - parameter A_S in (9)
 AKOP - parameter A_P in (9)
 AP0 - parameter σ_p in (9)
 SCRT - parameter σ_{crit} for the kinetic function ψ
 AN1 - parameter n in (9)
 SGC1 - parameter σ_* in (9)
 SGC2 - parameter σ_0 in (9)
 REC - parameter A_{c0} in (8)
 PRS0 - initial pressure in the material
 YST - fracture limit for the damage criterion

In order to specify the elastic moduli from the information above it should be noted that the bulk sound velocity is linked with the bulk modulus as $K = \rho_0 c_0^2$, and, similarly, for the shear modulus: $G = \rho_0 b_0^2$.

It should be noted that the present input data employs non-standard input units in *cm* (length), *g* (mass), $10\mu\text{sec} = 10^{-5}\text{sec}$ (time), and $^\circ\text{K}$ (temperature). The derived pressure unit in this case is GPa. At the end of the modifications, the initial values for the Poisson ratio,

and the bulk and shear moduli are calculated and initially checked in the same UINEP.FOR subroutine.

5.1.2 EOSVEI modifications

The EOS constants normally taken from an EOS analogue of the VP_data file should be replaced by the data specified within the UINEP input. However, the code uses the EOS data for initial calculation of mass arrays because the input of EOS data followed by the mass calculation is processed earlier than the elasto-plastic input. In order to use the input data correctly, when using the EOS identifier in the EOS section of the CTH input, we explicitly assign values of the initial density for the EOS model to be substituted, while leaving the remaining parameters of the EOS input intact.

5.1.3 UINCHK modifications

UINCHK.FOR modification includes a code fragment containing a new subroutine VEDCHK.FOR. The first part of the fragment arranges the definition of necessary types of the model allowing one to treat the model as the one, for which deviatoric stresses will be calculated. Then, a standard call to the subroutine SI2CTH introduces the unit transformation constants into a part of the input array VPUINP. Subsequent call of the VEDCHK subroutine transforms the constants into the CTH units from the non-standard input units, introduces global constants (the 'GC' part [17] of the array VPUINP) such as initial temperature T_0 and numerical limiting constants for the calculation of constitutive equations, and fills in the 'DC' part of the array with several derived constants used for EOS and CE calculations. This subroutine also calculates the constants a_k and b_k characterizing rate sensitivity of yield limits for the phases and recalculates auxiliary constants for the subsequent EOS calculations. After the VEDCHK call, the last part of the code fragment checks if the assigned MODLEP number for the present constitutive model is in agreement with the substituted EOS number MEQ [17] and fills in the EOS input data array used in EOS calls later on.

In order to allow for the deviatoric and bulk response decoupling, subroutines available for an EOS one-component VE model are replaced by the subroutines representing the present EOS (13) or (15). Therefore, an identifier previously used for the model from the CTH EOS-database in an EOS section of the CTH input is now used for the present model. Thus, the identifier and any dummy material name from the available material database for CTH's VE model identify the EOS model described in Section 3.

5.1.4 UINISV modifications

UINISV.FOR modifications make two calls for a standard subroutine MIGSEX [17] setting up default values for extra variables and for a new subroutine VEDEXV. The subroutine VEDEXV sets up the following extra variables: the damage parameter c (variable CC), strain deviator proportional to $(J_\sigma)^{1/2}$ (variable DEV), entropy variable at previous time cycle (ENT), structural force q (AEC), and the variable of density at the preceding time cycle (ROO). The variables are declared to be scalar with the selection of proper values for ITYPE (see [17]). Dimensions of the variables are adjusted appropriately with proper

choice of the array RDIM [17]. Initial values of the extra variables are defined via the pre-given array RINIT [17].

5.1.5 EOSVEK modifications

The extra variables defined in subsection 5.1.4 by UINISV are duplicated by a set with the same characteristics used for EOS calculations. This set is defined in the EOSVEK subroutine corresponding to the VE model. This set is updated at every time cycle with the values of the extra variables determined in the Lagrangian Block subroutine. This set is required because of the inability to directly access the EOSMRE subroutine dealing with the EOS extra variables.

5.2 Lagrangian Block

For the Lagrangian Block of the code, one subroutine ELSG [15-17] is involved in the modifications.

5.2.1 ELSG modifications

Modifications to the ELSG subroutine are the main driving part of the constitutive model. This part processes the equations taken in the standard form [18] for the Jaumann derivative to describe evolution of the stress tensor. Constitutive equations for description of the evolution of the deviatoric part of the stress tensor (10) are an analogue of the fourth equation of the system (3) of the model. The first part of the modifications in ELSG extracts the stress deviators at an old time step and the strain rate increments at the advanced half time step [18]. Next, new subroutine VEDSIG is called via the VEDDRV subroutine called in the main ELSG body. The subroutine calculates new stress deviators and the damage parameter. To do so, the subroutine first calls subroutine VEDEXD that calculates eigenvalues of the stress deviator tensor utilized in the damage criterion (17), elastic moduli (7), their derivatives over c required for calculation of the structural forces (4) (subroutine VEDMOD), and the damage parameter c . Then, the subroutine VEDSIG calculates the stress deviators in accordance with the strain deviator increments similarly to the constitutive equations (5) or (6), while ignoring the relaxation right-hand terms. Thus, an intermediate stress deviator s_{ij}^* is calculated. Next step deals with the stress reduction due to relaxation. For calculation of the scaling factor of the stress deviator, equation (6) is reduced to the following one for the parameter s where $s^2 = s_{ij} s_{ij}$:

$$\frac{ds}{dt} = -G \left(\frac{1-c}{G_1 \tau_1} + \frac{c}{G_2 \tau_2} \right) s = -Fs. \quad (18)$$

Here, the functions $\tau_k(s)$ are determined in (12). The equation (18) is discretised as follows

$$\frac{s^{n+1} - s^*}{\Delta t} = -F(s^{n+1}) s^{n+1}, \quad (19)$$

where Δt is the time increment and s^* is calculated from the intermediate stress deviator s^*_{ij} . The new value of the parameter s^{n+1} is calculated from (19) by iteration, using Newton's method within the body of subroutine VEDRLX called by VEDSIG. The stress deviators are calculated afterwards in the standard fashion:

$$s^{n+1}_{ij} = (s^{n+1} / s^n) \cdot s^n_{ij} .$$

5.3 Eulerian Remap Block

The third and last modification in the Eulerian Remap Block deals with the EREB subroutine [15].

5.3.1 EOSVEV and EOSVES modifications

The duplicate extra variable set defined in EOSVEK (subsection 5.1.5) can be used in EOS subroutines that are called from the EREB subroutine. Access to the EOS subroutines is available only through the VE model subroutines (parts of the EOS group of subroutines) that calculate the necessary pressure, temperature, and energy parameters along with their derivatives required by the code from (13) or (15). The modified subroutines differ only by their input and output sets. The EOSVEV subroutine needs density and internal energy (along with the extra variables) as input and calculates pressure and temperature. In turn, the EOSVES subroutine needs density and temperature as input and calculates pressure and internal energy. To use the present EOS (8) in these subroutines, entropy is replaced by temperature from (6). The invariant J_e is taken from the strain deviator variable of the extra variables set.

5.3.2 EOSVEX modifications

Using the internal energy updated on the Eulerian Remap step, the subroutine EOSVEX calculates entropy and density at the advanced time step. The modification utilizes the quadratic equation (8) with respect to S and updates the corresponding extra variables.

5.3.3 EREB modifications

These modifications deal with EOS calculations during the Eulerian remap step. In order to properly use the extra variable of strain deviator, $D = J_e$, a modification to the EREB subroutine includes calculation of D^{n+1} from the remapped values of s^{n+1}_{ij} and density ρ^{n+1} entering the shear modulus G according to the following formula used for (13):

$$D^{n+1} = s^{n+1}_{ij} \cdot s^{n+1}_{ij} / (2\rho^{n+1}G^{n+1})^2 ,$$

where G is taken from (16, 18). Because the EOS block employs its own extra variable array, the extra variables of the Lagrangian Block are updated by duplication of the Eulerian Extra Variables set into the Lagrangian set at the end of the EREB subroutine. These modifications to the Eulerian Remap module finalise implementation of the model.

6. Numerical examples

Two typical examples of damage response are considered below in two numerical CTH calculations using the implemented model. The first example, which is typical for glasses [9, 11-12] and some polymers, manifesting the brittle behavior at high strain rate loads such as polycarbonate [19], demonstrates development and propagation of fracture waves [9] where damage is initiated by a pressure rise.

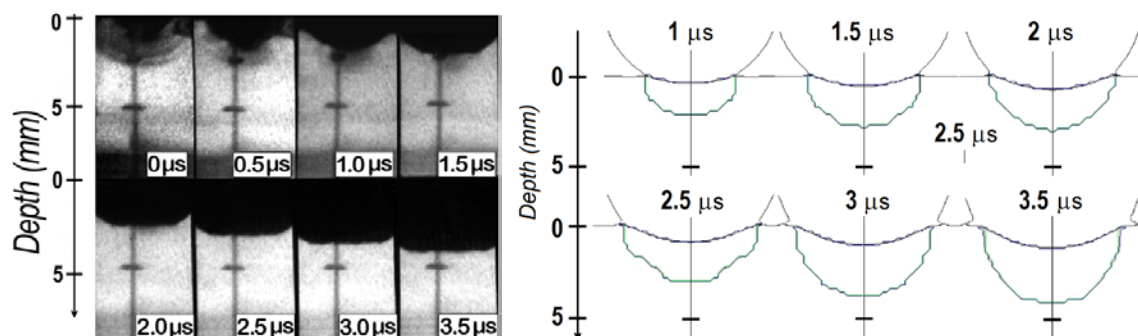


Fig. 1. Experiment (left) and CTH calculation (right) of the fracture wave propagation in glass subject to a high-velocity impact by a hemi-spherically nosed copper projectile at impact velocity of 536 m/s.

High-speed photographic images of the experiments [9] corresponding to this set-up are shown in Fig. 1 (left). The experimental results represent a high-velocity impact of a block of Pyrex glass by a hemi-spherically nosed copper projectile with an impact velocity of 536 m/s. These images demonstrate the remarkable effect of flattening the observed front of the fracture wave. LS-Dyna simulations [9] employing the present model describe the process well. The present simulation attempts to reproduce the results [9] using the present CTH implementation. Mechanical and elastic characteristics used for the glass are similar to those from [9] and are described in Section 3. Other parameters critical to the calculation are the damage mode indicators that emphasize the stress mode responsible for damage initiated either by pressure (dominating parameter A_p) or by shear (dominating parameter A_s). For the present case of glass we have selected $A_s = 0.3$ and $A_p = 0.9$ as specified above. It is seen that the damage zone calculated with the CTH hydrocode (Fig. 1, right) correlates with that observed in the experiments. In the present calculation, as seen from the ratio between the parameters A_s and A_p , the pressure mode dominates, which is mostly associated with the damage parameter accumulation due to pressure via the kinetic (17).

The next example describes the response of a concrete target due to a high velocity impact by a hard projectile within the frame of set-up [8]. This set-up represents a high velocity impact by a 197 g steel projectile against a 10 cm thick concrete target with an impact velocity of 308.4 m/s. Experimental results observed for recovered targets (e.g. [8, 20]) demonstrate a consistent damage pattern typical for the shear stress loading mode with

large spallation zone in the frontal area, similar scabbing at the distal side, and small damage in the middle of the target.

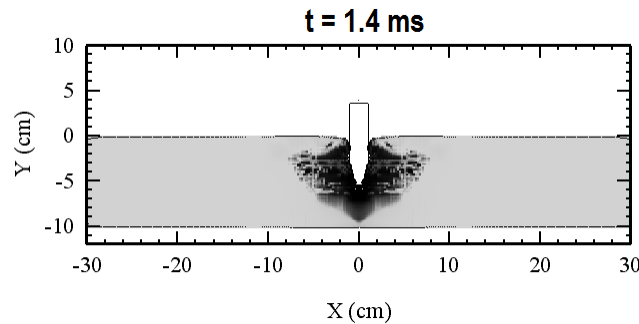


Fig. 2. The damage zones obtained with PSDam model.

However, when simulating the experiments within the abovementioned set-up, using the PSDam model [5] with material parameters corresponding to a plain concrete, the required damage pattern cannot be captured as seen in Fig. 2, although the material strength associated with the compression mode is selected almost as twice high as the strength associated with the shear mode (i.e., the value of a material constant of the PSDam model responsible for the shear strength was selected to be essentially lower than that for the compressive strength). Specifically, the damage areas of spalling and scabbing in the vicinity of the target interfaces at the projectile entry and exit are vanishingly small, and the major damage is concentrated in the middle section of the target as seen in Fig. 2. The situation is rather typical for many damage models as seen from the simulation results [7] that demonstrate a similar damage pattern for ballistic penetration of a concrete slab. This behaviour does not seem to be realistic with a low strength concrete when considering the interference of rarefaction waves at the free surfaces of target. At the same time, the compressive strength is essentially higher in the middle area affected by the projectile penetration. Therefore, a larger damage area in the middle of the target for the calculation shown in Fig. 2 seems to be unrealistic as well.

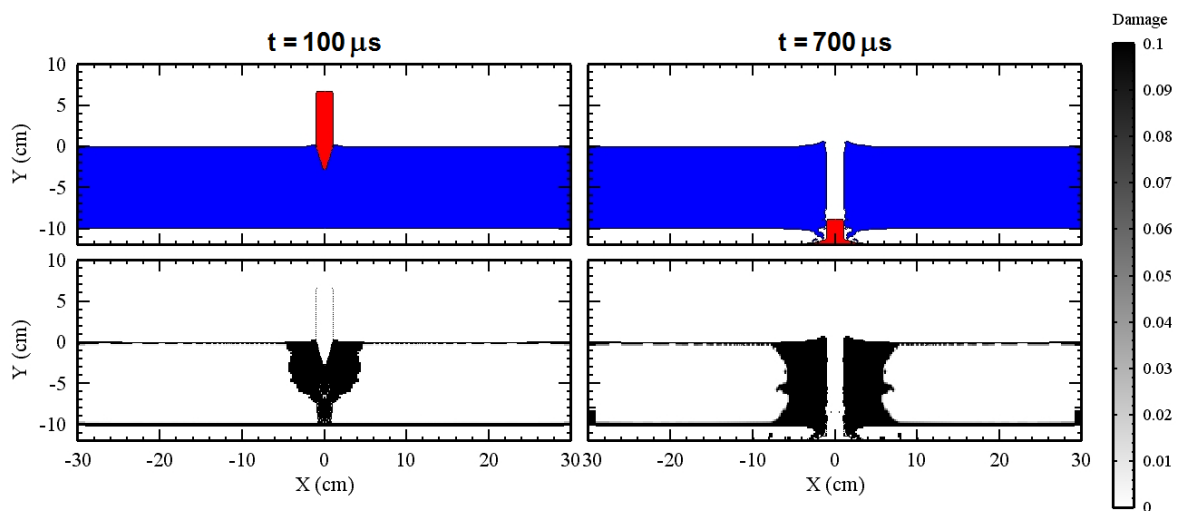


Fig. 3. Calculated damage zones obtained with the present CTH implementation of the model (the shear mode of damage is chosen for the concrete material).

Using the present CTH implementation of the damaged material model within the same set-up, we choose constants $A_S = 1$ and $A_P = 0$ as specified above in Section 4 for the concrete material, which enables the criterion (17) to associate fracture with the shear mode of loading. Results of the CTH simulation are shown in Fig. 3 and it is seen that this mode of fracture better predicts the experimental observations [8, 20] with a larger frontal and distal damage zones when compared with that in the middle section of the target. Thus, the simulation results shown in Fig. 3 demonstrate that the experimental pattern is reproduced more realistically following the shear mode domination in the model.

7. Conclusions

Preference of the CTH hydrocode to other codes is necessitated by the Eulerian set-up requirements enabling the code to process large deformations and by a large CTH material model database. These requirements are critical for evaluation of the weapons performance and countermeasure effectiveness.

The rate sensitive model taking damage accumulation into account [9] has been implemented in CTH using the bulk-shear decoupling [13] of the mechanical response.

Numerical examples simulated with the present CTH implementation have demonstrated the ability of the model to describe both shear- and pressure-dominated damage modes of fracture.

8. References

1. R.L. Bell, M.R. Baer, R.M. Brannon, D.A. Crawford, M.G. Elrick, E.S. Hertel, Jr., R.G. Schmitt, S.A. Silling, and P.A. Taylor, CTH user's manual and input instructions version 7.1, Sandia National Laboratories, Albuquerque, NM, 2006.
2. T.J. Holmquist, G.R. Johnson, W.H. Cook, A computational constitutive model for concrete subjected to large strains, high strain rates and high pressures, In: Proc. 14th Int. Symp. on Ballistics, Quebec, Canada, 1993, pp. 591-600.
3. S.A. Silling, Brittle Failure Kinetics Model for Concrete, Sandia report SAND97-0439C, Sandia National Laboratories, Albuquerque, NM, 1997.
4. S.A. Silling, CTH Reference Manual: BFK Model for Concrete, Sandia report SNL-NM, Sandia National Laboratories, Albuquerque, NM, 2001, draft.
5. R.M. Brannon, The Consistent Kinetics Porosity (CKP) Model: A Theory for the Mechanical Behavior of Moderately Porous Solids, Sandia report SAND2000-2696, Sandia National Laboratories, Albuquerque, NM, 2000.
6. P.A. Taylor, CTH Reference Manual: The Pressure Shear Damage (PSDam) Model, Sandia report SAND2003-0539, Sandia National Laboratories, Albuquerque, NM, 2003.
7. M. Polanco-Loria, O.S. Hopperstad, T. Børvik, and T. Berstad, Numerical predictions of ballistic limits for concrete slabs using a modified version of the HJC concrete model, *Int. J. Imp. Eng.*, 2008, 35, pp. 290-303.
8. T. Børvik, M. Langseth, O.S. Hopperstad, and M.A. Polanco-Loria, Ballistic perforation resistance of high performance concrete slabs with different unconfined compressive strengths, In: Proc. 1st Int. Conf. on High Performance Structures and Composites, ed. by C.A. Brebbia and W.P. de Wilde, Sevilla, Spain: WIT press (ISBN 1-85312-904-6), 2002, p. 273-282.
9. A.D. Resnyansky, E.I. Romensky, and N.K. Bourne, Constitutive Modeling of Fracture Waves, *J. App. Physics*, 2003, 93 (3), pp. 1537-1545.
10. J.O. Hallquist, D.W. Stillman, and T.-L. Lin, LS-DYNA3D User's Manual, Livermore Software Technology Corporation, Livermore, CA, 1994.
11. A.D. Resnyansky and N.K. Bourne, Kinetic Behaviour of Failure Waves in a Filled Glass, CP955, Shock Compression of Condensed Matter - 2007, ed. by M. Elert, M.D. Furnish, R. Chau, N. Holmes, and J. Nguyen, 2007, American Institute of Physics, pp. 255-258.
12. A.D. Resnyansky and N.K. Bourne, Ballistic impact of a hard projectile against a block of glass, In: Proc. 21st Int. Symp. on Ballistics, 2004, Australia.
13. A.D. Resnyansky, Thermodynamically Consistent Decoupled Shear-Volumetric Strain Model and CTH Implementation, DSTO report DSTO-TR-2299, Defence Science and Technology Organisation, Edinburgh, Australia, 2009.

14. S.K. Godunov and E.I. Romenskii, "Elements of Continuum Mechanics and Conservation Laws", Kluwer Academic Publ., N.Y., 2003.
15. E.P. Fahrenthold and C.H. Yew, Hydrocode simulation of hypervelocity impact fragmentation, *Int. J. Impact Eng.*, 1995, 17(1-3), pp. 303-310.
16. T.N. Dey, An effective model for dynamic finite difference calculations, Los Alamos National Laboratory Report LA-13093-MS, UC-703, Los Alamos, NM, 1996.
17. R.M. Brannon and M.K. Wong, MIG version 0.0 model interface guidelines: Rules to accelerate installation of numerical models into any compliant parent code, Sandia National Laboratories Report SAND96-2000, UC-405, Unlimited Release, Albuquerque, NM, 1996.
18. D.J. Benson, The Numerical Simulation of the Dynamic Compaction of Powders, In: *High-Pressure Shock Compression of Solids IV: Response of Highly Porous Solids to Shock Loading*, edited by L.W. Davison, Y. Horie, and M. Shahinpoor, Springer-Verlag, 1997, pp. 233-255.
19. A.D. Resnyansky, N.K. Bourne, and E.N. Brown, The Taylor Cylinder Response of PC and PMMA, *AIP Conf. Proc.* 1979, 2018, pp. 070026-1-070026-6.
20. S.J. Hanchak, M.J. Forrestal, E.R. Young, and J.Q. Ehrgott, Perforation of Concrete Slabs with 48 Mpa (7 Ksi) and 140 Mpa (20 Ksi) Unconfined Compressive Strengths, *Int. J. Imp. Eng.*, 1992, 12(1), pp. 1-7.

UNCLASSIFIED

DEFENCE SCIENCE AND TECHNOLOGY GROUP DOCUMENT CONTROL DATA		1. DLM/CAVEAT (OF DOCUMENT)
2. TITLE CTH Implementation of a Two-Phase Material Model With Damage		3. SECURITY CLASSIFICATION (FOR UNCLASSIFIED LIMITED RELEASE USE (U/L) NEXT TO DOCUMENT CLASSIFICATION) Document (U) Title (U) Abstract (U)
4. AUTHOR(S) Anatoly D. Resnyansky		5. CORPORATE AUTHOR Defence Science and Technology Group PO Box 1500 Edinburgh South Australia 5111 Australia
6a. DST GROUP NUMBER DST-Group-TR-3539	6b. TYPE OF REPORT Technical Report	7. DOCUMENT DATE October 2018
8. TASK NUMBER N/A	9. TASK SPONSOR VCDF	10. RESEARCH DIVISION Weapons and Combat Systems Division
11. MSTC Energetic Systems and Effects		12. STC Warheads and Effects
13. SECONDARY RELEASE STATEMENT OF THIS DOCUMENT <i>Approved for public release</i> OVERSEAS ENQUIRIES OUTSIDE STATED LIMITATIONS SHOULD BE REFERRED THROUGH DOCUMENT EXCHANGE, PO BOX 1500, EDINBURGH, SA 5111		
14. DELIBERATE ANNOUNCEMENT No limitations		
15. CITATION IN OTHER DOCUMENTS Yes		
16. RESEARCH LIBRARY THESAURUS CTH hydrocode; Multi-phase constitutive modelling; Brittle materials; Damage; High-velocity Impact		
17. ABSTRACT A material model taking strength and damage accumulation into account is implemented in the CTH hydrocode. The model is based on a two-phase approach with the phases representing virgin and fully crushed material states with individual strength and elastic characteristics. Multi-phase description is realised via a homogenisation procedure representing a damaging material as a mixture of the phases, which results in an equation of state, constitutive equations, and conservation laws. The implementation has been used for numerical modelling of high velocity impact against targets made of generic materials representing glass and concrete. The calculations illustrate the dominating effect of the damage mode specified by material.		

UNCLASSIFIED